Towards Real-time SAR Measurement with MR Thermometry

Changqing Ye[1], An Jing[2], Yan Zhuo[1], Rong Xue[1], and Jing Chen[1]

[1]*State Key Laboratory of Brain and Cognitive Science, Beijing MRI Center for Brain Research, Institute of Biophysics, Chinese Academy of Sciences, Beijing, Beijing, China,* [2]*Siemens Mindit Magnetic Resonance Ltd., Shenzhen, Guangzhou, China*

Introduction: For ultra-high field imaging, many sequences are limited by the increased RF energy deposition into the subjects, which is conventionally quantified by Specific Absorption Rate (SAR). Currently, the SAR during scan is calculated by the pulse energy method, which can only estimate the global SAR and then further infer the local SAR. This method has two drawbacks. First, it is an indirect estimation method, therefor scan subject's safety cannot be guaranteed. Second, in case that SAR is over estimated, unnecessary scan limitations will occur. In this work, we present a PRF-based MR thermometry method to supervise the RF energy deposition directly with real-time temperature measurement.

Theory and Methods: ***Requirements of Temperature Map:*** According to FDA Guidelines for Magnetic Resonance Equipment Safety, [1] the temperature increase should be less than 1℃ in human brain. To accurately monitor the temperature change within 1℃, the precision of MR thermometry must be 0.1℃ or higher. To approach real-time measurement the total acquisition time for each temperature measurement should be less than 10 seconds, hence repeating measurement every 5-min only increase the total scan time by 3%. Based on SAR simulation in previous studies, [2-4] the local hotspot could be as small as 13 mm*14 mm*15 mm. To catch this local SAR increase, image resolution of 3.4x3.4x3.4 mm3 would be sufficient, in which case covering the hotspot with more than 60 voxels.

Precision of PRF-based thermometry: For PRF method, $\Delta T = \frac{\Delta\varphi}{\gamma\alpha B_0 TE}$ (1), and $\delta_{\Delta T} = \frac{\delta_{\Delta\varphi}}{\gamma\alpha B_0 TE} = \frac{\sqrt{2}}{\gamma\alpha B_0 TE}\frac{1}{SNR}$ (2), where $\delta_{\Delta T}$ and $\delta_{\Delta\varphi}$ is the standard deviation of the temperature map and phase difference image, respectively. As shown in Equation (1) and (2), the temperature change is calculated by the temperature-dependence phase difference and the precision of the temperature map ($\delta_{\Delta\varphi}$) is inversely proportional to SNR. [5] To verify Eq.2, a simulation result is compared to the measured data in a tofu phantom. The precision was calculated by the spatial standard deviation of the temperature values in a region containing 10,000 voxels, without temperature variation or signal inhomogeneity. The phantom was imaged on 3T Siemens Tim Trio system using a GRE sequence (TE1/TE2/TR=20/50/100 ms, FOV=128×128 mm^2, matrix =128×128, slice thickness=2 mm) and flip angle was varied from 15 to 45 to achieve different SNR in the temperature maps.

Real-time temperature map with high-SAR sequence: To verify the temperature increase induced by a high-SAR sequence, the following experiment was implemented in an agar gel phantom on 7T Siemens Magnetom system with a Nova medical volume transmit and 24-ch receive coil. A short repetition TSE sequence was used as high-SAR sequence with total scan time of 3:18 min and SAR=100%, which is the largest allowable SAR value on scanner for first level controlled mode (4W/kg). For the PRF method, single shot EPI was used with the following parameters: TE/TR=30/2000 ms, FOV=160×160 mm^2, resolution= 2.5×2.5×3.5 mm^3, number of slices=21, TA=2 s. To verify the temperature increasing, four thermo-optic probes (AccuSens; OpSens, Quebec, Canada) were placed into the phantom as shown in Fig.2 (P1, P2, P3, P4). Probe 3 was located near the middle of the phantom and was used as a reference to remove the phase drift. [5] More detail on this issue is included in the discussion section. In the experiment, a phase map was first acquired with ss-EPI as the baseline. Next, the high SAR TSE was applied 3 times continuously, each time immediately followed by an ss-EPI-based PRF temperature measurement.

Results: As shown in Fig.1, the precision is inversely proportion to SNR at two different TEs, which agree with the simulation of Eq.2. According to Eq.2, on 7T with TE=30 ms, a SNR over 30 could provide a temperature precision higher than 0.1℃. Fig.2 shows evolution of the temperature map of the center slice as the high-SAR sequence was applied continuously. At the locations where probes were inserted, the values of the temperature map is consist with the values recorded by the thermo-optic probes. Such as, at 10th min, the values of temperature map (probes) are 0.10℃, 0.19℃, 0.08℃ (0.07℃, 0.17℃, 0.11℃), respectively. The largest difference between temperature map and probe measurement is 0.03℃ across the whole experiment.

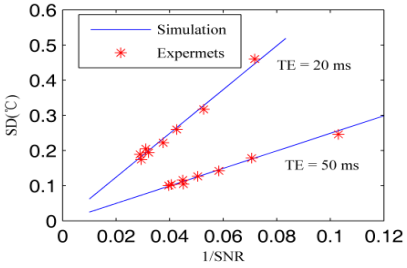

Fig.1. Simulation of equation (2) and experimental data points. They match with each other very well.

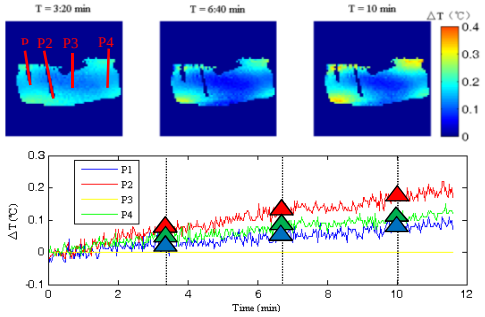

Fig.2. Temperature increase map (top). Temperature recorded by the thermo-optic probes (bottom). The values showed by triangle were measured on temperature map at the location of probes. They show good consistency with the value of the probes.

Conclusion and Discussions: In this work, we show that temperature increased by the RF energy deposition can be measured by PRF thermometry method with a very high precision (<0.1℃) within a very short time (2 s) with reasonable spatial resolution (2.5×2.5×3.5 mm^3) and coverage (160×160×73 mm^3). This method might be used to monitor temperature change in subjects directly, which would be especially useful for ultra-high field imaging. In our experiments, a global phase drift was observed without any temperature change, which would introduce a global phase error in the temperature measurements. To avoid the phase error, probes 3 was used as the reference and assume to be at constant temperature throughout the scan. Therefore, the temperature maps in Fig.2 are actually temperature difference maps. Our future work includes correcting phase drift over time by other more reliable methods, for example, a fat phantom could be used to as the constant reference, linear plane fit method and PRF combined with Diffusion method. [6]

References: 1. Loren A. Zaremba. FDA Guidelines for Magnetic Resonance Equipment Safety, Center for Devices and Radiological Health, Food and Drug Administration; 2. Kozlov, M. and R. Turner. Fast MRI coil analysis based on 3-D electromagnetic and RF circuit co-simulation. JMR. 2009; 200(1):147-152; 3. Wang, Z., et al. SAR and temperature: simulations and comparison to regulatory limits for MRI. J Magn Reson Imaging, 2007; 26(2): 437-441; 4. Collins, C.M., et al. Temperature and SAR calculations for a human head within volume and surface coils at 64 and 300 MHz. J Magn Reson Imaging, 2004;19(5):650-656; 5. Ishihara, Y., et al. A precise and fast temperature mapping using water proton chemical shift. Magn Reson Med 1995; 34(6): 814-823; 6. Rieke, V. and K. Butts Pauly, MR thermometry. J Magn Reson Imaging, 2008; 27(2):376-390.

Acknowledgements: This work was supported by CAS (KSCX2-YW-R-259), MOST (2012CB825500, 2012IM030100), NSFC (90820307, 81271567).